Title

Simulations of Nanoblade-Enhanced Laser-Induced Cathode Emissions and Analyses of Yield, MTE, and Brightness

Authors

Mann, J
Lawler, G
Rosenzweig, J B
et al.

Publication Date

2021

DOI

10.18429/JACoW-IPAC2021-WEPAB147

ISBN: 978-3-95450-214-1 ISSN: 2673-5490 doi:10.18429/JACoW-IPAC2021-WEPAB147

SIMULATIONS OF NANOBLADE-ENHANCED LASER-INDUCED CATHODE EMISSIONS AND ANALYSES OF YIELD, MTE, AND BRIGHTNESS*

J. Mann†, G. Lawler, J. B. Rosenzweig, UCLA, Los Angeles, CA, USA
J. K. Nangoi, T. Arias, Cornell University, Ithaca, NY, USA

Abstract

Laser-induced field emission of electrons from metallic nanotips has been well studied. Unfortunately, nanotips suffer low damage thresholds with enhanced fields around 10 GV/m. The nanoblade, akin to a nanotip extruded in one lateral dimension, may reach upwards of 40 GV/m due to its robust thermomechanical properties. This increased surface field promises brighter electron emissions. We perform simulations of strong-field emissions from metallic nanoblades via the 1-D time-dependent Schrödinger equation with effective Jellium and nonlinear collective image charge potentials, including the strong field gradients induced by the nanostructure. We measure spectra and yields and compare to recent experiments. Potential analytical forms of image potential limited yield for a spectrally rich emission are presented. Calculations of mean transverse energy are provided as well as a prospective method of mitigation with the goal of increasing brightness.

INTRODUCTION

The ever-growing field of nanostructured cathodes has seen applications in electron microscopes [1], ultra-fast (low energy) electron diffraction [2], and electron guns in general [3]. The most common structure, the nanotip, benefits from an emission area on the scale of 10s of nm. However, the tip is limited in the peak enhanced surface field that may be achieved by material breakdown at fields on the order of 10 GV/m [4, 5]. The goal of increasing brightness may be progressed by a similar nanostructure. The nanoblade, which is essentially an extruded nanotip, has superior thermomechanical properties to the nanotip while supplying sufficient field enhancement to be compatible with tabletop lasers. These benefits allow for peak fields upwards of 40 GV/m, and potentially up to 80 GV/m [6, 7] providing large yields in a space-charge limited regime.

To further understand this photoemitter we perform a 1-D time-dependent Schrödinger equation (TDSE) simulation of the metallic surface of the nanoblade including a self-consistent image potential to model space-charge limited yield. We are currently working on several methods of calculating weights for the initial states in this 1-D system to more accurately coincide with the tunneling capability of each state in a real material. These weights will be summarized in a general-purpose material normal energy distribution (MNED). But, as this analysis is in its infancy, we will proceed by using a free electron gas (FEG) model. We provide two analytical models for the space-charge limited yield, applicable for spectrally rich emissions. With these results we estimate two primary mean transverse energy (MTE) contributions from this emitter. We then propose a method of improving brightness.

TDSE SIMULATION

We model the metallic surface of the nanoblade by a Jellium slab with surface potential using Eq. (3) in Ref. [8]. We additionally apply a polynomial smooth spline to vacuum at the rear of our slab over 100 nm to minimally reflect retrograde free electrons while maintaining a finite system.

The initial electron states are taken to be the eigenstates from the bottom of the Jellium slab well ($-W - E_f$) up to the Fermi level ($-W$). We equate each 1-D state to a slice of the Fermi sphere to determine its 3-D density contribution.

We include the geometry of our emitter by a mixed 1-D to 3-D projection model. In the field the effective Hartree potential (HP) is calculated with the electron density representing infinitely long cylinders, with radius measured from R within the Jellium slab. Within the slab the HP is calculated as though field electrons are cylindrical and internal electrons are planar.

The simulation is propagated using the operator-splitting Fourier method with Strang splitting. The external laser field is modeled with a spatial profile provided from a finite-difference time-domain calculation of gold (including the penetrating field), enhancement factor of about 4, and a Gaussian temporal envelope.

SIMULATION RESULTS

Running the simulation with the HP yields the electron density as a function of time shown in Fig. 1. The laser pulse envelope is centered about 80 fs with a peak strength of 40 GV/m, wavelength of 800 nm, and pulse full-width half-max-power of 8 fs. We model gold with $W = 5.1$ eV and $E_f = 5.53$ eV.

Electrons that are ionized propagate towards the upper boundary with some encountering an image potential turning point before they are absorbed at the boundary. Some electrons that escape would encounter a turning point further on indicating the need for a proceeding simulation to model the transport far away from the cathode.

Closed trajectories appearing near the surface ($x = 0$) at about $t = 120$ fs are due to reflections from the slab backing. As these trajectories are confined to the slab and return to

* This research was funded by the Center for Bright Beams, National Science Foundation Grant No. PHY-1549132.
† jomann@physics.ucla.edu

ISBN: 978-3-95450-214-1 ISSN: 2673-5490 doi:10.18429/JACoW-IPAC2021-WEPAB147

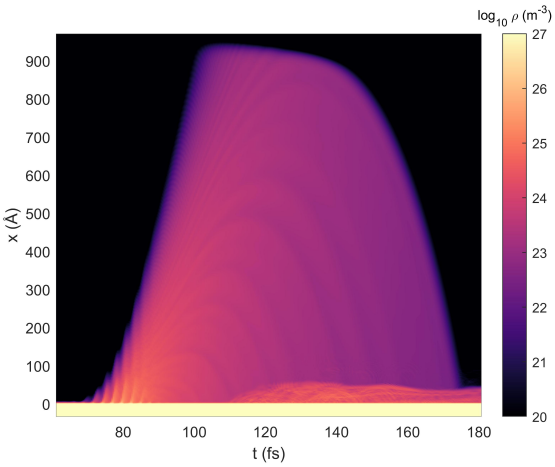

Figure 1: Time-dependent electron density for a 40 GV/m field simulation with HP included.

the surface after the pulse is complete they have no effect on emission statistics.

Some sample spectra are shown in Fig. 2. Both moderate (20 GV/m) and strong (40 GV/m) field simulations show suppression due to the image potential in the lower harmonics. This effect is exacerbated for larger fields. We also note that, without the HP, the peaks in the spectra are spaced by the laser frequency, 1.5 eV. In the 40 GV/m case this spacing is preserved for rescattered electrons but stretched to about 3 eV for direct electrons. This showcases the importance of the HP on the low energy emissions whereas the rescattered high energy emissions are largely unaffected by escaping before substantial space-charge is accumulated.

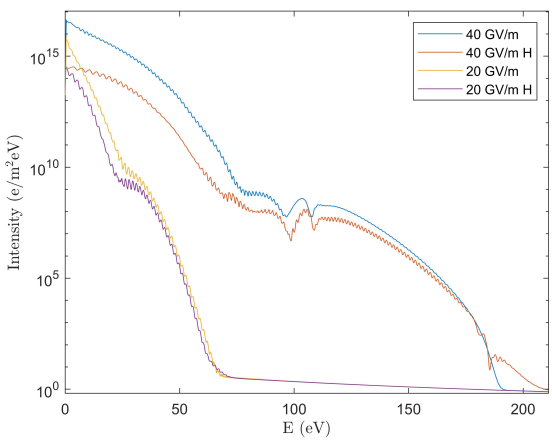

Figure 2: Sample emission spectra from the TDSE with the HP at 40 (orange) and 20 (purple) GV/m and without the HP at 40 (blue) and 20 (yellow) GV/m.

Yield curves with and without the HP are shown in Fig. 3. The associated power laws agree well for the low-field behavior, with a scaling power of about 3.5. With $W = 5.1$ eV and $\hbar\omega = 1.55$ eV we expect the low field exponent to follow the photon order of 4, so this is consistent as a moderate-field result. In the strong-field, beyond the "kink" around 10^{13} W/cm^2, the power law without the HP reduces to about 2.3 via channel closing while the HP result is further suppressed to an exponent of about 1.3.

We expect the power law to approach a linear intensity relation for strong fields [6]. Further propagating the output of this simulation in a semi-classical manner to the detector, using a far-field non-infinite cylindrical charge model, may result in this linear behavior as we are overestimating the yield.

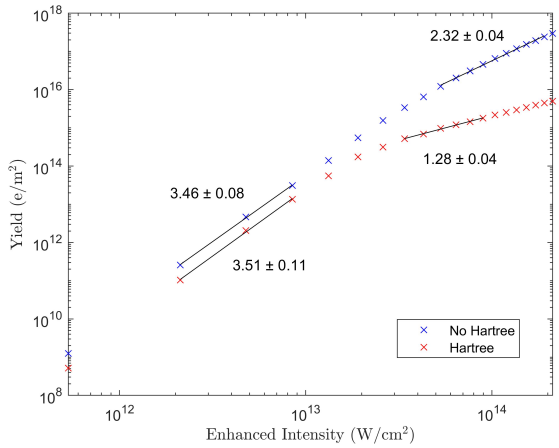

Figure 3: Yield curves with (red) and without (blue) the HP. Power law exponents determined by fits to select data points are shown.

MODELS FOR SPACE-CHARGE LIMITED YIELD FROM BROADBAND SOURCES

A straightforward approach to finding a space-charge limited yield for zero-energy emission is to equate the near-field ponderomotive force to the collective image potential force. However, with emissions at several eV, this analysis may not be applicable, especially around this regime transition.

Instead let us treat the collective image potential as a perfect high-pass spectral filter. The image potential will permit electrons to emit above a threshold and recaptures them below that threshold energy. We generalize by letting the total image potential be $V = -N\phi(I)$ where N is the number of ultimately emitted electrons and $\phi(I)$ is the approximately constant potential contribution of each electron. We will consider two possible regimes.

Image Potential Spans the Direct Spectrum

If the image potential remains within the direct part of the spectrum, $< 2U_p$, then the electron distribution is effectively exponential. By equating the cutoff energy to the image potential and comparing the number of electrons emitted we arrive at the yield

$$N = \frac{\sigma(I)}{\phi(I)} W_0\left(a\frac{\phi(I)}{\sigma(I)} I^b\right), \quad (1)$$

ISBN: 978-3-95450-214-1 ISSN: 2673-5490 doi:10.18429/JACoW-IPAC2021-WEPAB147

where $\sigma(I)$ is the spectral decay rate as a function of the laser intensity, b is the low-field yield power law scaling, a is a scaling factor for the spectrum, and W_0 is the Lambert W function. Experiments [6] show that yields should tend towards a linear function of I whereas this equation approaches $N = \frac{\sigma(I)}{\phi(I)} \ln\left(a\frac{\phi(I)}{\sigma(I)} I^b\right)$, necessitating complicated forms for σ and/or ϕ.

Image Potential Spans the Plateau

If the image potential is deep enough that it affects electrons in the plateau we may treat the relevant spectrum as roughly flat. With this model we get that $N = \frac{aI^{b-1}E_f(I)}{1+aI^{b-1}\phi(I)}$ with $E_f(I)$ being an effective cutoff energy to ensure finite total yield. For the strong-field results to match experiments we require that $\frac{E_f}{\phi}(I) = I$.

MTE DUE TO SOURCE DISTRIBUTION

Here we will assume that the electrons are sourced from a FEG. The simulation provides 1-D yield as a function of the initial parallel momentum, $\eta(k_\parallel)$. The MTE may be calculated by summing up the transverse energy contributions over the Fermi sphere and normalizing by the yield

$$MTE_s = \frac{\hbar^2}{4m} \frac{\int dk_\parallel (k_f^2 - k^2)^2 \eta(k_\parallel)}{\int dk_\parallel (k_f^2 - k^2) \eta(k_\parallel)}. \quad (2)$$

Applying this formula to our results provides the MTE curves in Fig. 4. The MTE ranges from about 250 meV for low fields to 700 meV near 40 GV/m. Fortunately the MTE relates to the intensity logarithmically with and without the HP while yield scales at least linearly, so increasing the enhanced intensity still leads to brighter emissions considering this MTE contribution.

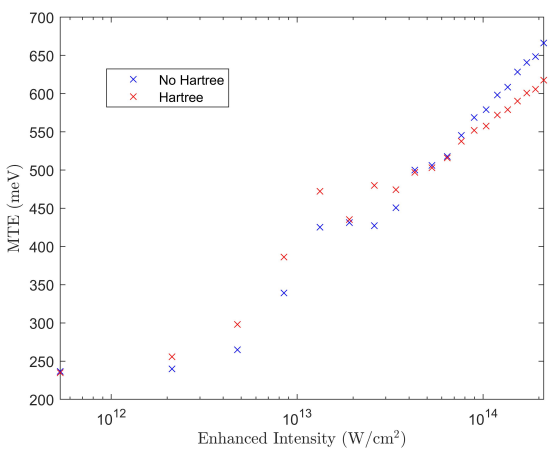

Figure 4: The source distribution MTE with (red) and without (blue) the HP as a function of enhanced laser intensity.

MTE DUE TO SURFACE CURVATURE

Another source of MTE is due to the curvature of the blade. As the field is not perfectly confined to the apex we see emissions with eV-scale normal energy spreading over a large angle. Given an angle-dependent spectrum $f(E, \theta)$ the MTE is

$$MTE_c = \frac{\int\int d\theta dE\, E \sin^2\theta f(E,\theta)}{\int\int d\theta dE\, f(E,\theta)}. \quad (3)$$

In one extreme, with uniform field profiles across the blade edge and bounded by $\pm\theta_{max}$, we get $MTE_c \approx \frac{1}{2}(1 - \text{sinc}\ 2\theta_{max})\langle E\rangle_0$ with $\langle E\rangle_0$ the average normal emission energy, typically a few eV. We estimate this MTE to be up to several eV at high fields. Reducing this MTE and improving brightness would require reducing the effective angular spread or filtering out larger energies.

Maximizing Brightness for Surface Curvature

Since the plateau cutoff scales with the field strength, which decreases away from the apex, we may decrease the emission spread by filtering out lower energy emissions. Specifically we will filter out electrons below $E_0 - \Delta E$, with E_0 the maximal plateau energy and ΔE the energy window size. Expressing the plateau cutoff as a power law of the field, $E_0(\theta) = a\mathscr{E}^\gamma(\theta)$, and assuming the field profile decays locally like $\mathscr{E}(\theta) = (1 - b\theta^\alpha)\mathscr{E}$ we get a maximal angle of $\theta_{max} \approx \left(\frac{\Delta E}{ab\gamma\mathscr{E}^\gamma}\right)^{1/\alpha}$.

Then we overestimate the MTE by assuming the plateau does not retreat off-apex, plugging these forms into Eq. (3), and taking the expansion's lowest order in θ_{max} we get that

$$MTE_c \approx E_0 \frac{1+\alpha}{3+\alpha}\theta_{max}^2 \propto \Delta E^{2/\alpha}, \quad (4)$$

and with the yield $N \propto \theta_{max}\Delta E \propto \Delta E^{1+1/\alpha}$ we get a 6-D brightness of $B \propto \Delta E^{-1/\alpha}$. As $\alpha > 0$ we will improve brightness by decreasing our window size. Of course this will eventually conflict with the intrinsic metallic MTE and the single electron emission limit. Further work may reveal an optimal window size. Another possible method may be a low-pass filter where we only take the lowest energies.

CONCLUSION

We have performed TDSE calculations modeling electronic emissions from metallic nanoblades illuminated by a strong pulsed laser. We include an effective Hartree potential to partially model the collective image charge force of the emissions to show a transition to space-charge limited yield. We estimate the intrinsic metallic MTE to be 100's meV and the MTE due to nanostructure curvature to be up to several eV. This may be somewhat mitigated by spectrally filtering the emissions. Future work includes progress on the MNED, space-charge models with exchange-correlation potentials, and post-TDSE classical simulations.

REFERENCES

[1] R. Bormann, S. Strauch, S. Schäfer, and C. Ropers, "An ultrafast electron microscope gun driven by two-photon photoemission from a nanotip cathode", *Journal of Applied Physics*, vol. 118, no. 17, p. 173 105, 2015. doi:10.1063/1.4934681

ISBN: 978-3-95450-214-1 ISSN: 2673-5490 doi:10.18429/JACoW-IPAC2021-WEPAB147

[2] G. Storeck, S. Vogelgesang, M. Sivis, S. Schäfer, and C. Ropers, "Nanotip-based photoelectron microgun for ultrafast leed", *Structural Dynamics*, vol. 4, p. 044 024, 2017. doi:10.1063/1.4982947

[3] B. Schröder, M. Sivis, R. Bormann, S. Schäfer, and C. Ropers, "An ultrafast nanotip electron gun triggered by grating-coupled surface plasmons", *Applied Physics Letters*, vol. 107, no. 23, p. 231 105, 2015. doi:10.1063/1.4937121

[4] M. Krüger, C. Lemell, G. Wachter, J. Burgdörfer, and P. Hommelhoff, "Attosecond physics phenomena at nanometric tips", *Journal of Physics B: Atomic, Molecular and Optical Physics*, vol. 51, p. 172 001, Aug. 2018. doi:10.1088/1361-6455/aac6ac

[5] R. Bormann, M. Gulde, A. Weismann, S. V. Yalunin, and C. Ropers, "Tip-enhanced strong-field photoemission", *Phys. Rev. Lett.*, vol. 105, p. 147 601, Sep. 2010. doi:10.1103/PhysRevLett.105.147601

[6] T. Paschen *et al.*, "Near-field-driven electron rescattering at a nanoblade", unpublished.

[7] G. Lawler, J. Mann, V. Yu, and J. Rosenzweig, "Initial nanoblade-enhanced laser-induced cathode emission measurements", presented at the 12th Int. Particle Accelerator Conf. (IPAC'21), Campinas, SP, Brazil, May 2021, paper WEPAB097, this conference.

[8] P. J. Jennings, R. O. Jones, and M. Weinert, "Surface barrier for electrons in metals", *Phys. Rev. B*, vol. 37, pp. 6113–6120, Apr. 1988. doi:10.1103/PhysRevB.37.6113